Condensed Matter and Interphases
(Kondensirovannye sredy i mezhfaznye granitsy)

Original articles

DOI: https://doi.org/10.17308/kcmf.2020.22/3115
Received 20 August 2020
Accepted 07 October 2020
Published online 25 December 2020

ISSN 1606-867X
eISSN 2687-0711

Synthesis, Microstructural and Electromagnetic Characteristics of Cobalt-Zinc Ferrite

© 2020 A. I. Goryachko✉, S. N. Ivanin, V. Yu. Buz'ko

Kuban State University,
14, Stavropolskaya str., Krasnodar 350040, Russian Federation

Abstract

In this study, cobalt-zinc ferrite ($Co_{0.5}Zn_{0.5}Fe_2O_4$) was obtained by the glycine-nitrate method followed by annealing in a high-temperature furnace at a temperature of 1300 °C. The qualitative composition and its microstructural characteristics were determined using energy-dispersive X-ray spectroscopy, X-ray diffraction analysis, and scanning electron microscopy.

The analysis of the micrographs demonstrated that the cobalt-zinc ferrite micropowder obtained after thermal annealing has an average particle size of 1.7±1 μm. The analysis of XRD data showed that the annealed cobalt-zinc ferrite micropowder has a cubic crystal structure with a lattice parameter of a = 8.415 Å. Using the Scherrer and Williamson-Hall equations we calculated the average sizes of the coherent scattering regions, which were commensurate with the size of crystallites: according to the Scherrer equation D = 28.26 nm and according to the Williamson-Hall equation D = 33.59 nm and the microstress value $\varepsilon = 5.62\times10^{-4}$ in the ferrite structure.

Using a vector network analyser, the electromagnetic properties of a composite material based on synthesized cobalt-zinc ferrite were determined. The frequency dependences of the magnetic and dielectric permeability values from the measured S-parameters of the composite material (50% ferrite filler by weight and 50% paraffin) were determined using the Nicolson-Ross-Weir method and were in the range of 0.015–7 GHz. The analysis of the graphs of the dependence of the magnetic permeability on the frequency of electromagnetic radiation revealed a resonance frequency of $f_r \approx 2.3$ GHz. The discovered magnetic resonance in the UHF range allows the obtained material to be considered as being promising for use as an effective absorber of electromagnetic radiation in the range of 2–2.5 GHz.

Keywords: glycine-nitrate synthesis, cobalt-zinc ferrite, ferrimagnetic, microstructure, composite materials, magnetic permeability, dielectric permittivity.

For citation: Goryachko A.I., Ivanin S.N., Buz'ko V. Yu. Synthesis, microstructural and electromagnetic characteristics of cobalt-zinc ferrite. *Kondensirovannye sredy i mezhfaznye granitsy = Condensed Matter and Interphases*. 2020; 22(4): 446–452. DOI: https://doi.org/10.17308/kcmf.2020.22/3115

Для цитирования: Горячко А. И., Иванин С. Н., Бузько В. Ю. Синтез, микроструктурные и электромагнитные характеристики кобальт-цинкового феррита. *Конденсированные среды и межфазные границы*. 2020; 22(4): 446–452. DOI: https://doi.org/10.17308/kcmf.2020.22/3115

✉ Goryachko Alexander Ivanovich, e-mail: Alexandr_g_i@mail.ru

1. Introduction

The development of methods for obtaining powder metal-oxide magnetic materials is currently considered an urgent task. Such materials are ferrites, which are solid solutions based on iron (III) oxide [1–3]. It is known, that zinc-based ferrite spinels are often used in the industry. The main ones are manganese-zinc and nickel-zinc ferrites with a cubic crystal lattice. However, the disadvantage of these ferrites is their rather low resonance frequency. The substitution of cobalt or nickel by manganese allows the magnetic properties to be changed significantly, namely, to shift the resonance to higher frequencies and, consequently, to increase Snoek's limit [4].

Now, there are various methods for obtaining both nano-sized and micro-sized ferrite powders using ceramic technologies and from salt solutions [5–7]. The production method significantly affects the shape and size of the particles, which determines the microstructural and electromagnetic properties of the material [8–10]. For example, one of the most widespread methods of obtaining ferrite powder is ceramic synthesis [11–14]. However, the disadvantage of this method is the long-term high-temperature annealing, which leads to an inhomogeneity of particles, the manifestation of anisotropy, and the poor reproducibility of electromagnetic properties; therefore, chemical syntheses are promising methods for obtaining ferrite materials. When ferrite is obtained by chemical synthesis, energy consumption can be reduced and the uniformity of particles can be significantly improved [15]. The main chemical methods for producing ferrites from metal nitrates include: nitrate-urea [16, 17], nitrate-citrate [18, 19], as well as the glycine-nitrate method used in this study [20–22], etc. The advantage of the glycine-nitrate method is that the required temperature of the mixture at which the pyrochemical reaction occurs is about 150 °C, which is significant lower than that of nitrate-urea and nitrate-citrate syntheses.

The purpose of this study was the synthesis of cobalt-zinc ferrite by the glycine-nitrate method, high-temperature annealing at a temperature of 1300 °C, and research into its microstructural and electromagnetic characteristics.

2. Experimental

The following reagents were used for the synthesis of $Co_{0.5}Zn_{0.5}Fe_2O_4$ ferrite: $Co(NO_3)_2 \cdot 6H_2O$ (chemically pure, RF), $Zn(NO_3)_2 \cdot 6H_2O$ (chemically pure, RF), $Fe(NO_3)_3 \cdot 9H_2O$ (analytical grade, RF), glycine acid ($C_2H_5NO_2$, chemically pure, RF). The metal nitrates and glycine that were used were taken in the required stoichiometric quantities and then dissolved in bi-distilled water. Then the resulting mixture was gradually heated for 1 h to a temperature of 150 °C with constant stirring. After a certain amount of time, after the evaporation of the excess volume of bi-distilled water, the solution was a viscous gel-like product. With further heating, the resulting viscous gel ignited spontaneously, followed by combustion for 5–6 seconds. In the course of thermolysis, a highly porous, weakly magnetic, light brown foamy substance was formed. The equation for the pyrochemical reaction that took place can be represented as follows:

$$0.5Co(NO_3)_2 \cdot 6H_2O + 0.5Zn(NO_3)_2 \cdot 6H_2O + 2Fe(NO_3)_3 \cdot 9H_2O + 3C_2H_5NO_2 \rightarrow Co_{0.5}Zn_{0.5}Fe_2O_4 + 5.5N_2\uparrow + 6CO_2\uparrow + 37.5H_2O\uparrow + 0.25O_2\uparrow$$

After the completion of the reaction and subsequent cooling, the ferrite sample was ground in a ceramic mortar for 30 minutes. Then, for the removal of the residual impurities, the resulting synthesized powder was heat treated in a "Nabertherm Top 16/R + B400" high-temperature furnace at a temperature of 1300 °C for 1 hour. Additionally, after cooling, the calcined ferrite powder was ground in a ceramic mortar for 10 minutes in order to obtain a homogeneous micropowder.

Photos of the microstructure of the investigated $Co_{0.5}Zn_{0.5}Fe_2O_4$ ferrite were obtained using a "JEOL JSM-7500F" scanning electron microscope and energy dispersive analysis was performed using the "INCA X-Sight" attachment.

X-ray diffraction analysis of the cobalt-zinc ferrite sample was carried out using a "Shimadzu XRD-7000" powder diffractometer. The sample was investigated at room temperature in the angle range of 2θ from 3° up to 70° with a scanning step of 0.02°.

For the study of the electromagnetic properties of cobalt-zinc ferrite, a composite material based on paraffin with a ferrite filler concentration of 50% by weight was made.

The sample was made in the form of a toroid with a thickness of 4 mm, an outer diameter of 7 mm, and an inner diameter of 3.05 mm. Electromagnetic characteristics (magnetic and dielectric constants) were calculated based on experimentally measured S-parameters using a "Deepace KC901V" vector network analyser in the range of 0.015-7 GHz.

3. Results and discussion

The spectrum of energy dispersive X-ray spectroscopy (EDS) with the selected analysis area for the studied $Co_{0.5}Zn_{0.5}Fe_2O_4$ ferrite micropowder, annealed for 1 hour at a temperature of 1300 °C is shown in Fig. 1. The obtained results of the EDA analysis show the presence of the main elements: Co (12.68%), Zn (12.24%), Fe (45.21%) and O (29.86%) in the composition of the studied micropowder.

The photograph of an annealed $Co_{0.5}Zn_{0.5}Fe_2O_4$. micropowder is presented in Fig. 2a. Based on the analysis of the obtained photograph, it can be noted that after thermal annealing at a temperature of 1300 °C the studies sample consisted of spherical microparticles. The detailed examination of the microstructure of the powder revealed both individual and fused ferrite particles. Based on the analysis of the micrographs of the studied $Co_{0.5}Zn_{0.5}Fe_2O_4$, the histogram of the particle size distribution depending on their number was calculated (Fig. 4b). The histogram of the particle size distribution was obtained based on the analysis of 2700 particles using the "ImageJ" program. For each individual particle, the equivalent diameter was determined based on the results of measurements of its length and width according to the procedure from the study [23]. Based on the data obtained from the histogram of annealed $Co_{0.5}Zn_{0.5}Fe_2O$ ferrite a relatively narrow particle size distribution was revealed. The calculated average particle size of the synthesized cobalt-zinc ferrite is 1.7 ± 1 μm, which indicates a high degree of particle homogeneity in the studied sample.

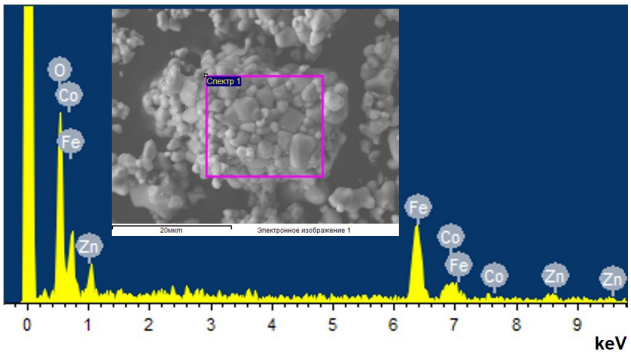

Fig. 1. EDX spectrum of the studied $Co_{0.5}Zn_{0.5}Fe_2O_4$ ferrite annealed at a temperature of 1300 °C

The XRD pattern for the investigated $Co_{0.5}Zn_{0.5}Fe_2O_4$ ferrite micropowder is presented in Fig. 3, and the processed data of XRD pattern are presented in Table 1.

Analysis of the obtained data demonstrates that the characteristic peaks on the XRD pattern correspond to the pure cubic spinel phase [24]. Using equation (1), it was determined that the annealed ferrite micropowder has a cubic structure with a crystal lattice parameter of a = 8.415 Å. The calculated parameter of the

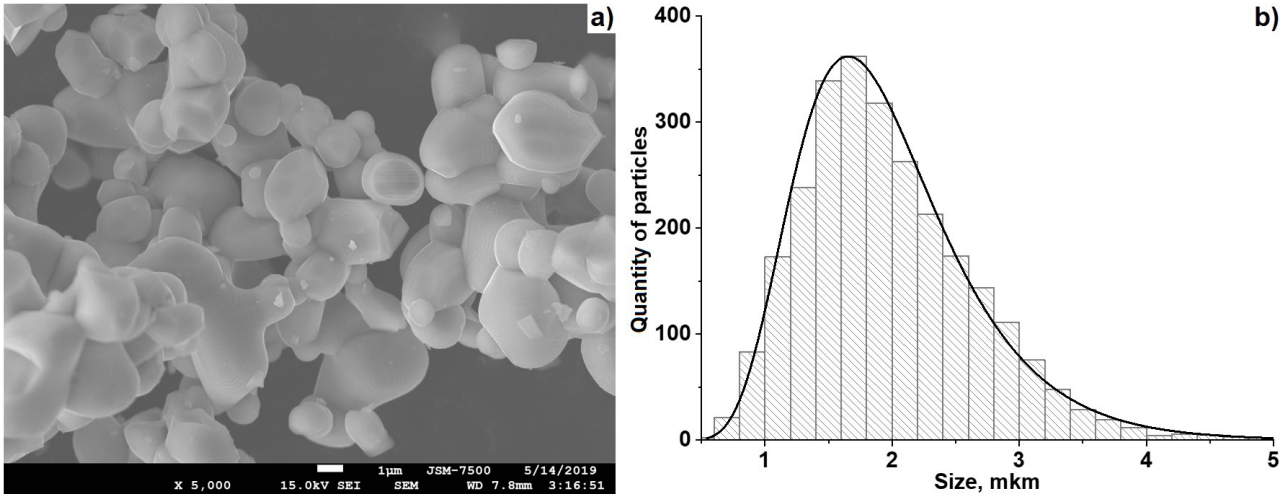

Fig. 2. SEM micrograph of the studied powder at a magnification of ×5000 (a) and a histogram of the particle size (b), for $Co_{0.5}Zn_{0.5}Fe_2O_4$ after annealing for 1 hour at a temperature of 1300 °C

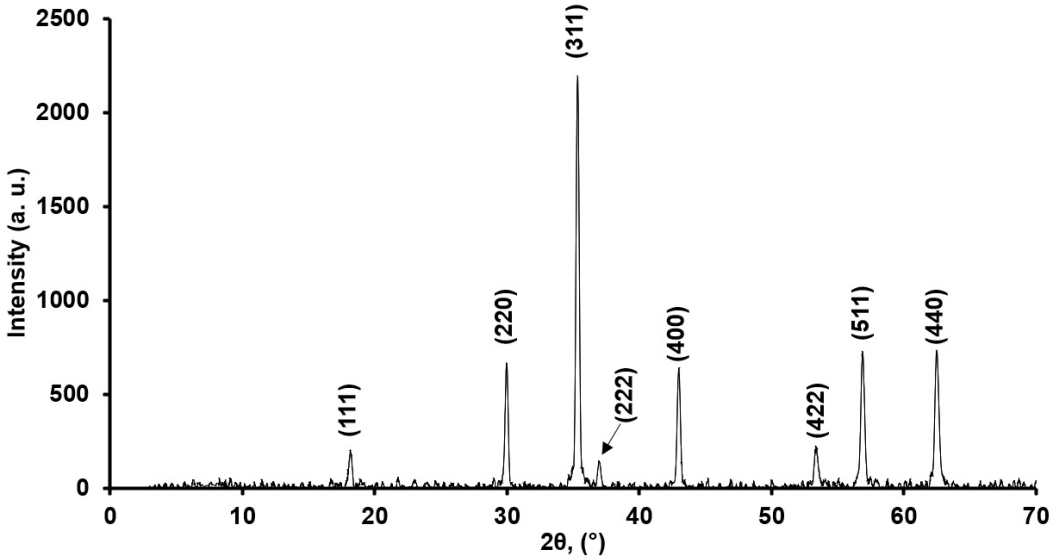

Fig. 3. XRD pattern of the investigated $Co_{0.5}Zn_{0.5}Fe_2O_4$ micropowder after annealing for 1 hour at a temperature of 1300 °C

Table 1. XRD data for the investigated $Co_{0.5}Zn_{0.5}Fe_2O_4$ ferrite

no. of peak	angle, 2θ	Intensity, [%]	d-spacing, [Å]	FWHM, rad
1	18.18	9.6	4.876	0.00489
2	29.98	29.6	2.978	0.00471
3	35.36	100	2.536	0.00488
4	36.96	7.6	2.430	0.00488
5	43.00	20.3	2.102	0.00506
6	53.34	8.1	1.716	0.00617
7	56.90	26	1.617	0.00610
8	62.48	34.3	1.485	0.00612

crystal lattice for the investigated ferrite agrees well to the data of the study [25] demonstrating that a = 8.418 Å, for $Co_{0.5}Zn_{0.5}Fe_2O_4$ ferrite after 6-hour annealing at 1000 °C [25].

$$\frac{1}{d_{hkl}^2} = \frac{(h^2 + l^2 + k^2)}{a^2}. \quad (1)$$

Average size of coherent scattering regions (CSR) – D, comparable with the crystallite size, was calculated for the sample based on the data of X-ray diffraction analysis (XRD) using the Scherrer equation (2) [19]:

$$D = \frac{k\lambda}{\beta\cos\theta}. \quad (2)$$

Where k = 0.9 for spherical particles; λ = 0.154 – wavelength of CuK_α radiation, nm; β – half-width at half-heights of integral peaks, rad, θ –Bragg angle, rad.

The CSR value calculated according to Scherrer for the investigated ferrite is: D = 28.26 nm.

Additionally for the investigated ferrite, the CSR values and microstresses were calculated using Williamson-Hall method (Fig. 3) according to equation (3):

$$\text{FWHM}\cdot\cos\theta = \frac{\lambda}{D} + 4\varepsilon\cdot\sin\theta, \quad (3)$$

where FWHM is the half-width at half-height of the integral peaks, rad; θ — Bragg angle, rad; λ = 0.154 – wavelength of CuK_α radiation, nm; D – the required size of the CSR, nm; ε – microstress value.

Calculation of CSR sizes and microstresses for $Co_{0.5}Zn_{0.5}Fe_2O_4$ micropowder by Williamson–Hall method provided the following results: CSR size – 33.59 nm, which insignificantly differs from the data obtained by the Scherrer method; microstress value $\varepsilon = 5.62\times10^{-4}$.

The values of the magnetic ($\mu = \mu' + i\mu''$) and dielectric ($\varepsilon = \varepsilon' + i\varepsilon''$) permittivity in complex form for a composite material based on the

investigated $Co_{0.5}Zn_{0.5}Fe_2O_4$ were calculated from the experimentally measured values of S_{11} and S_{21} according to the Nicholson–Ross–Weir algorithm [26–29]. The tangents of the angles of magnetic and dielectric losses were calculated using the following formulas (4):

$$\mathrm{tg}\,\delta_\mu = \frac{\mu''}{\mu'},\ \mathrm{tg}\,\delta_\varepsilon = \frac{\varepsilon''}{\varepsilon'} \quad (4)$$

Fig. 4a shows the graphs of the dependence of μ′ and μ″ for the investigated composite material ($Co_{0.5}Zn_{0.5}Fe_2O_4$/paraffin = 1/1 by weight) in the frequency range of 0.015–7 GHz. A slight decrease in μ′ from 1.85 to 1.69 was observed in the low frequency range (0.015–0.5 GHz). However, with an increase in the frequency of electromagnetic radiation (> 0.5 GHz), the significant sharp decrease in μ′ value up to 1.041 at frequency of 7 GHz can be seen on the graph. The analysis of μ″ data revealed that the maximum value of the magnetic loss was observed at the frequency of f_r ≈ 2.3 GHz, which is in good agreement with the data of [30], where the maximum value of magnetic losses is observed in the range of 2.2–2.4 GHz [30]. Maximal detected μ″, which was 0.323, corresponded to the resonance frequency for the produced composite material. Based on the obtained μ′ and μ″ data, tangent of the angle of magnetic losses at the resonant frequency was calculated and it was tg δ_μ ≈ 0.252.

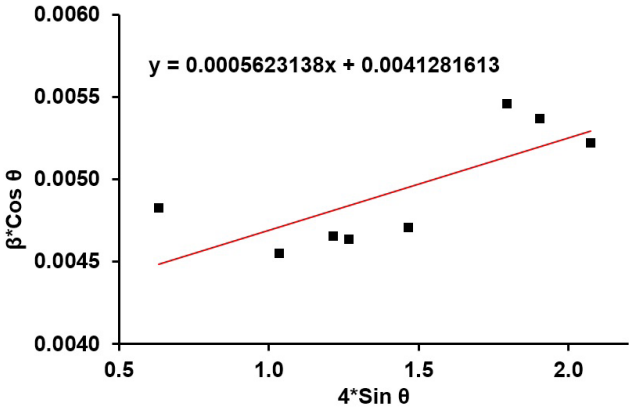

Fig. 4. Williamson-Hall plot for the investigated $Co_{0.5}Zn_{0.5}Fe_2O_4$

Dependency graphs of ε′ and ε″ for the manufactured composite material based on $Co_{0.5}Zn_{0.5}Fe_2O_4$ are shown in Fig. 4b. According to the experimental data, it can be seen that the value for both ε′ and ε″ for the investigated composite sample practically does not change in the entire investigated frequency range, on the basis of which it can be concluded that the average value of the dielectric constant for cobalt-zinc ferrite in the investigated frequency range is ε′ ≈ 3.12 and ε″ ≈ 0.014. From the calculated date for ε′ and ε″ it follows that the tangent of the angle of dielectric losses in the entire measured range was tg δ_ε ≈ 0.0045.

Since the values obtained for ε′, ε″ and tg δ_ε were low and practically did not change in the entire investigated frequency range, it can be concluded that the dielectric parameters insignificantly affect the radio-absorbing (except for the resonance frequency shift) or radio-shielding characteristics of the investigated composite material.

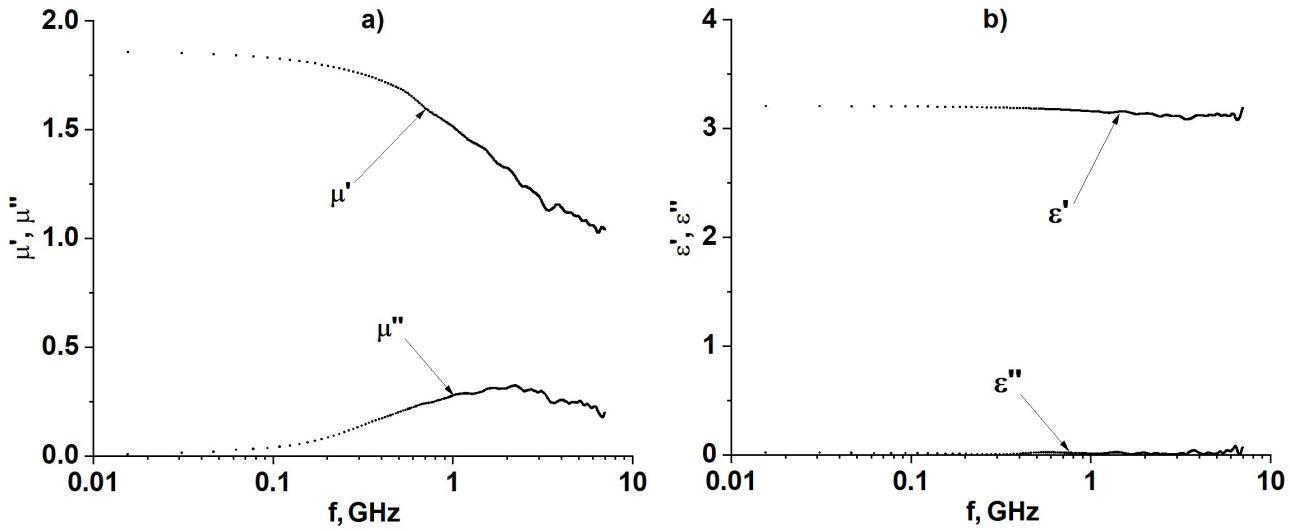

Fig. 5. Frequency dependence of complex magnetic permeability (a) and complex dielectric permittivity (b) for the fabricated composite material based on $Co_{0.5}Zn_{0.5}Fe_2O_4$

4. Conclusions

The granular ferrite $Co_{0.5}Zn_{0.5}Fe_2O_4$ with micron-sized granules consisting (according to XRD data) of nanocrystals with average sizes of ~25–35 nm was obtained by glycine-nitrate synthesis after one-hour thermal annealing at 1300 °C and subsequent grinding. The synthesized ferrite after thermal annealing did not contain impurities of other elements or side phases as was confirmed by EDS and XRD methods. Analysis of XRD data showed that investigated $Co_{0.5}Zn_{0.5}Fe_2O_4$ ferrite has a cubic crystal lattice. The resulting ferrite powder after high-temperature annealing of $Co_{0.5}Zn_{0.5}Fe_2O_4$ at 1300 °C within 1 hour has a fairly high uniformity in shape and particle size as was established based on the obtained micrographs and histograms of the particle size distribution. The analysis of the graphs of the dependence of magnetic permeability on the frequency of electromagnetic radiation revealed the magnetic resonance at frequency 2.3 GHz. The discovered magnetic resonance in the UHF range allows the obtained material to be considered as being promising for use as an effective absorber of electromagnetic radiation in the range of 2–2.5 GHz.

Acknowledgements

The work was carried out based on the REC Centre for Collective Use "Diagnostics of the structure and properties of nanomaterials" of the Kuban State University.

Conflict of interests

The authors declare that they have no known competing financial interests or personal relationships that could have influenced the work reported in this paper.

References

1. Thakur P., Chahar D., Taneja S., Bhalla N. and Thakur A. A review on MnZn ferrites: Synthesis, characterization and applications. *Ceramics International*. 2020;46(10): 15740–15763. DOI: https://doi.org/10.1016/j.ceramint.2020.03.287

2. Pullar R. C. Hexagonal ferrites: A review of the synthesis, properties and applications of hexaferrite ceramics. *Progress in Materials Science*. 2012;57(7): 1191–1334. DOI: https://doi.org/10.1016/j.pmatsci.2012.04.001

3. Kharisov B. I., Dias H. V. R., Kharissova O. V. Mini-review: Ferrite nanoparticles in the catalysis. *Arabian Journal of Chemistry*. 2019;12(7): 1234–1246. DOI: https://doi.org/10.1016/j.arabjc.2014.10.049

4. Stergiou C. Microstructure and electromagnetic properties of Ni-Zn-Co ferrite up to 20 GHz. *Advances in Materials Science and Engineering*. 2016;2016: 1–7. DOI: https://doi.org/10.1155/2016/1934783

5. Economos G. Magnetic ceramics: I, General methods of magnetic ferrite preparation. *Journal of the American Ceramic Society*. 1955;38(7): 241–244. DOI: https://doi.org/10.1111/j.1151-2916.1955.tb14938.x

6. Yurkov G. Y., Shashkeev K. A., Kondrashov S. V., Popkov O. V., Shcherbakova G. I., Zhigalov D. V., Pankratov D. A., Ovchenkov E. A., Koksharov Y. A. Synthesis and magnetic properties of cobalt ferrite nanoparticles in polycarbosilane ceramic matrix. *Journal of Alloys and Compounds*. 2016;686: 421–430. DOI: https://doi.org/10.1016/j.jallcom.2016.06.025

7. Karakaş Z. K., Boncukçuoğlu R., Karakaş İ. H. The effects of fuel type in synthesis of $NiFe_2O_4$ nanoparticles by microwave assisted combustion method. *Journal of Physics: Conference Series*. 2016; 707: 012046. DOI: https://doi.org/10.1088/1742-6596/707/1/012046

8. Shirsath S. E., Jadhav S. S., Mane M. L., Li S. *Handbook of sol-gel science and technology*. Springer, Cham.; 2016. p. 1–41. DOI: https://doi.org/10.1007/978-3-319-19454-7_125-1

9. Vyzulin S. A., Kalikintseva D. A., Miroshnichenko E. L., Buz'ko V. Y., Goryachko A. I. Microwave absorption properties of nickel–zinc ferrites synthesized by different means. *Bulletin of the Russian Academy of Sciences: Physics*. 2018;82(8): 943–945. DOI: https://doi.org/10.3103/s1062873818080439

10. Janasi S. R., Emura M., Landgraf F. J. G., Rodrigues D. The effects of synthesis variables on the magnetic properties of coprecipitated barium ferrite powders. *Journal of Magnetism and Magnetic Materials*. 2002;238(2-3): 168–172. DOI: https://doi.org/10.1016/s0304-8853(01)00857-5

11. Ahmed Y. M. Z. Synthesis of manganese ferrite from non-standard raw materials using ceramic technique. *Ceramics International*. 2010;36(3): 969–977. DOI: https://doi.org/10.1016/j.ceramint.2009.11.020

12. Mahadule R. K., Arjunwadkar P. R., Mahabole M. P. Synthesis and characterization of $Ca_xSr_yBa_{1-x-y}Fe_{12-z}La_zO_{19}$ by standard ceramic method. *International Journal of Metals*. 2013;2013: 1–7. DOI: https://doi.org/10.1155/2013/198970

13. Tarţa V. F., Chicinaş I., Marinca T. F., Neamţu B. V., Popa F., Prica C. V. Synthesis of the nanocrystalline/nnosized $NiFe_2O_4$ powder by ceramic method and mechanical milling. *Solid State Phenomena*. 2012;188: 27–30. DOI: https://doi.org/10.4028/www.scientific.net/ssp.188.27

14. Pradhan A. K., Saha S., Nath T. K. AC and DC electrical conductivity, dielectric and magnetic properties of $Co_{0.65}Zn_{0.35}Fe_{2-x}Mo_xO_4$ (x = 0.0, 0.1 and 0.2) ferrites. *Applied Physics A*. 2017;123(11): 715. DOI: https://doi.org/10.1007/s00339-017-1329-z

15. Low Z. H., Ismail I., Tan K. S. Sintering processing of complex magnetic ceramic oxides: A comparison between sintering of bottom-up approach synthesis and mechanochemical process of top-down approach synthesis. *Sintering Technology - Method and Application*. Malin Liu (ed.). 2018: 25–43. DOI: https://doi.org/10.5772/intechopen.78654

16. Costa A. C. F. M., Morelli M. R., Kiminami R. H. G. A. Combustion synthesis: Effect of urea on the reaction and characteristics of Ni–Zn ferrite powders. *Journal of Materials Synthesis and Processing*. 2001;9(6): 347–352. DOI: https://doi.org/10.1023/A:1016356623401

17. Maleknejad Z., Gheisari K., Raouf A. H. Structure, microstructure, magnetic, electromagnetic, and dielectric properties of nanostructured Mn–Zn ferrite synthesized by microwave-induced urea–nitrate process. *Journal of Superconductivity and Novel Magnetism*. 2016;29(10): 2523–2534. DOI: https://doi.org/10.1007/s10948-016-3572-5

18. Jalaiah K., Chandra Mouli K., Vijaya Babu K., Krishnaiah R.V. The structural, DC resistivity and magnetic properties of Mg and Zr Co-substituted $Ni_{0.5}Zn_{0.5}Fe_2O_4$. *Journal of Science: Advanced Materials and Devices*. 2018;4(2): 310–318. DOI: https://doi.org/10.1016/j.jsamd.2018.12.004

19. Yue Z., Zhou J., Li L., Zhang H., Gui Z. Synthesis of nanocrystalline NiCuZn ferrite powders by sol–gel auto-combustion method. *Journal of Magnetism and Magnetic Materials*. 2000;208(1-2): 55–60. DOI: https://doi.org/10.1016/s0304-8853(99)00566-1

20. Chick L. A., Pederson L. R., Maupin G. D., Bates J. L., Thomas L. E., Exarhos G. J. Glycine-nitrate combustion synthesis of oxide ceramic powders. *Materials Letters*. 1990;10(1-2): 6–12. DOI: https://doi.org/10.1016/0167-577x(90)90003-5

21. Salunkhe A. B., Khot V. M., Phadatare M. R., Pawar S. H. Combustion synthesis of cobalt ferrite nanoparticles—Influence of fuel to oxidizer ratio. *Journal of Alloys and Compounds*. 2012;514: 91–96. DOI: https://doi.org/10.1016/j.jallcom.2011.10.094

22. Martinson K. D., Cherepkova I. A., Sokolov V. V. Formation of cobalt ferrite nanoparticles via glycine-nitrate combustion and their magnetic properties. *Glass Physics and Chemistry*. 2018;44(1): 21–25. DOI: https://doi.org/10.1134/s1087659618010091

23. Kuzmin V. A., Zagrai I. A. A comprehensive study of combustion products generated from pulverized peat combustion in the furnace of BKZ-210-140F steam boiler. *Journal of Physics: Conference Series*. 2017;891: 012226. DOI: https://doi.org/10.1088/1742-6596/891/1/012226

24. Maleki A., Hosseini N., Taherizadeh A. Synthesis and characterization of cobalt ferrite nanoparticles prepared by the glycine-nitrate process. *Ceramics International*. 2018;44(7): 8576–8581. DOI: https://doi.org/10.1016/j.ceramint.2018.02.063

25. Waje S. B., Hashim M., Wan Yusoff W. D., Abbas Z. Sintering temperature dependence of room temperature magnetic and dielectric properties of $Co_{0.5}Zn_{0.5}Fe_2O_4$ prepared using mechanically alloyed nanoparticles. *Journal of Magnetism and Magnetic Materials*. 2010;322(6): 686–691. DOI: https://doi.org/10.1016/j.jmmm.2009.10.041

26. Nicolson A. M., Ross G. F. Measurement of the intrinsic properties of materials by time-domain techniques. *IEEE Transactions on Instrumentation and Measurement*. 1970;19(4): 377–382. DOI: https://doi.org/10.1109/tim.1970.4313932

27. Rothwell E. J., Frasch J. L., Ellison S. M., Chahal P., Ouedraogo R.O. Analysis of the Nicolson-Ross-Weir method for characterizing the electromagnetic properties of engineered materials. *Progress In Electromagnetics Research*. 2016;157: 31–47. DOI: https://doi.org/10.2528/pier16071706

28. Vicente A. N., Dip G. M., Junqueira C. The step by step development of NRW method. Proceedings Article in: *2011 SBMO/IEEE MTT-S International Microwave and Optoelectronics Conference (IMOC 2011). 29 Oct. – 1 Nov.* 2011. 738–742. DOI: https://doi.org/10.1109/imoc.2011.6169318

29. Ivanin S. N., Buz'ko V. Yu., Goryachko A. I., Panyushkin V. T. Electromagnetic characteristics of heteroligand complexes of gadolinium stearate. *Russian Journal of Physical Chemistry*. 2020;94(8): 1623–1627. DOI: https://doi.org/10.1134/S0036024420080130

30. Liu Y. W., Zhang J., Gu L. S., Wang L. X., Zhang Q. T. Preparation and electromagnetic properties of nanosized $Co_{0.5}Zn_{0.5}Fe_2O_4$ ferrite. *Rare Metals*. 2016. DOI: https://doi.org/10.1007/s12598-015-0670-7

Information about the authors

Goryachko Alexander Ivanovich, PhD student, Department of Theoretical Physics and Computer Technologies, Faculty of Physics and Technology, Kuban State University, Krasnodar, Russian Federation; e-mail: Alexandr_g_i@mail.ru. ORCID iD: https://orcid.org/0000-0001-6480-353X.

Ivanin Sergey Nikolaevich, PhD student, Kuban State University, Krasnodar, Russian Federation; e-mail: Ivanin18071993@mail.ru. ORCID iD: https://orcid.org/0000-0001-9352-5970.

Buzko Vladimir Yurievich, PhD in Chemistry, Associate Professor, Department of Radiophysics and Nanotechnology, Faculty of Physics and Technology, Kuban State University, Krasnodar, Russian Federation; e-mail: Buzkonmr@maul.ru. ORCID iD: https://orcid.org/0000-0002-6335-0230.

All authors read and approved the final manuscript.

Translated by Valentina Mittova
Edited and proofread by Simon Cox